The Variation of Core Loss in High-Frequency Transformers Under Different Load Conditions

Navid Rasekh, Jun Wang, Xibo Yuan
Department of Electrical and Electronic Engineering, University of Bristol
Bristol, United Kingdom
Email: Navid.Rasekh@Bristol.ac.uk; Jun.Wang@Bristol.ac.uk; Xibo.Yuan@Bristol.ac.uk

Keywords

«High-frequency power converter», «Transformer», «Core loss», «Iron losses», «Eddy current loss»

Abstract

Typically, the core loss of the high-frequency (HF) transformers is considered constant regardless of the load condition on the secondary side. This paper indicates that the various load conditions can affect the core loss in HF transformers due to the variation of winding parasitics elements and subsequently the transformer's excitation voltage and current waveforms, and the field interactions between the primary and secondary windings and between the windings and core. The contribution of this work is demonstrating the core loss variation depending on different load conditions in HF transformers, which is not commonly assessed and considered in previous studies. The captured experimental results are compared with the three-dimensional (3D) finite element analysis (FEA) results conducted in Ansys Maxwell, to provide a better comprehension.

I. Introduction

Power converters are largely composed of different types of high-frequency (HF) transformers which are a key component in these such systems. The core loss of HF transformers is an essential parameter to characterize in converter design and enables accurately optimising the system specifications. In order to determine transformer losses, empirically measurement methods with potentially higher accuracy are widely used instead of the analytical methods. There is a great deal of literature on the core loss measurement approaches under sinusoidal excitations at the no-load test [1]. In contrast, not much has been done on measuring transformer core loss in high-frequency PWM excitation under different load conditions, or on practical issues and errors analysis related to these measurements.

In recent years, pulse-width modulation (PWM) converters have evolved toward higher switching frequencies along with the development of wide-bandgap power devices. A challenge for PWM converters has been to estimate precisely the core loss of magnetic components at high frequencies. Instead of sinusoidal excitation, in PWM converters, an HF transformer is exposed to rectangular voltage and different shapes of excitation current such as triangular, depending on various applications, which can affect the core loss. Since the transformers' core datasheets and analytical equations are based on sinusoidal excitation, calculating the core loss value in these methods is not accurate enough in the case of PWM converters [2-5]. Another challenge regarding obtaining the core loss is the dc bias factor, which is also called pre-magnetization and indicates the position of the *B–H* loop in relation to the origin, where $H_0 = 0$. The core loss of the magnetic components is reported to be impacted significantly by different dc biased currents [2-3], [5]. To sum it up, the analytical and direct schemes methods based on impedance or network analyzer (small-signal measurement) are not entirely suitable to obtain the transformer core loss [1], [6]. For that reason, experimentally measuring the core loss in a large signal is preferred compared to the other methods for achieving higher accuracy in the loss evaluation.

For the conventional power transformers with sinusoidal excitation, the core loss is carried out empirically with an open circuit or no-load test [7]. In this test, the transformer is excited from the low voltage (LV) side with the rated voltage/frequency, and the high voltage (HV) side is left open. As a

result, power does not transfer from primary to secondary, and no current passes through the secondary winding. The generated flux in the core becomes the rated value, and the no-load current is quite small about 2 % to 10 % of the rated current during the test [8]. Accordingly, the wattmeter on the LV side records both the core and the LV winding losses. In spite of this, the winding loss is negligible compared with the loss in the core; because firstly, the frequency is low and the parasitic elements of the winding are negligible, and secondly, the core flux is in the rated value and the magnetizing current is insignificant.

In contrast, the advancement of power converter technologies enables intelligent and feasible operation at higher frequencies. At the same time, various modulation controls and distortions in current and voltage waveforms compared to the traditional sinusoidal excitation transformers may occur and impact the core loss. For instance, the dual active bridge (DAB) is an ideal choice at high frequencies for applications requiring high power density. The required HF transformer act as a magnetic link stage to transfer power between the two bridges, while the modulation control of DAB affects the waveform of flux distribution. As a consequence, the core loss estimation by traditional approaches becomes inaccurate if the flux varies due to the involvement of different types of switching patterns and excitation waveforms. For an example of core loss variation, the core loss of the HF transformers decreases by increasing the inner phase shift ratio of the excitation voltage in the dual-phase shift (DPS) modulation [9].

Additionally, as reported in previous high-frequency non-sinusoidal studies such as [9], with different load conditions, the voltage and current waveforms' shapes of the HF transformer are altered under light or heavy loads, which may, in turn, affect the core loss similar to the previous case. When a load presents in an HF transformer, the secondary winding conducts a current, and the primary current, as well as the field interactions between the windings or the mutual resistances, are changed compared to the no-load condition. Consequently, the winding loss will be changed accordingly due to the proximity effect [10-12]. On top of that, changing the AC resistance can influence the end/edge-winding leakage flux, and causes a local flux density variation in the edge of the core region, which leads to a change in the core loss as reported in [13]. Furthermore, depending on the application, the winding loss can also vary owing to phase shift between primary and secondary windings currents caused by the proximity effect on the different load conditions [14]. Similarly, this phase shift changes the winding resistances and alters the magnetic field distribution between the primary and secondary windings and also field interaction between the core and windings, which can subsequently change the core loss. Therefore, a precise empirical method with the same excitation waveforms and presence of the load used in the real test is needed to find these additional impacts on the HF transformer core loss, rather than a simplified no-load and small-signal tests.

Typically, the core loss of the HF transformers is considered constant regardless of the load conditions on the secondary side. This paper indicates that the presence of the load in the circuit can change the core loss value compared to the no-load condition. The core loss of the HF transformer is measured with the well-known two-winding method in the two conditions, i.e. the no-load and loaded. The load value is also varied to better investigate its impact on the core loss. Hence, The contribution of this work is demonstrating the core loss variation depending on different load conditions in an HF transformer, which is not commonly assessed and considered in previous studies. The captured experimental results are compared with the three-dimensional (3D) finite element analysis (FEA) results conducted in Ansys Maxwell, to provide a better comprehension.

II. Empirical HF Transformer Core Loss Measurement

A. No-Load Condition

The two-winding method is commonly used to measure the core loss of the HF transformers empirically as depicted in Fig. 1 [1-5], [15-17].

In this method, the secondary of the transformer is kept open and the primary winding is excited with the desired voltage and frequency. When the secondary winding is open-circuited and disconnected from the load, it does not conduct a current ($i_{Sec} = 0$). However, there is a nonzero current flowing through the primary winding as excitation current (i_{Exc}) and flows all the time during the operation of

the transformer, which is assumed to be independent of the secondary load. The excitation current, which is equal to the primary current (i_{Pri}) for the no-load condition, is the summation of the core loss resistance (R_C) current, i_C, and the magnetizing inductance (L_M) current, i_M. Therefore, a part of the excitation current is used to create flux in the transformer core as i_M, and another part is required to overcome hysteresis and eddy current losses of the transformer core as i_C. The i_C is largely in phase with the supply voltage (V_{Pri}) while the i_M lags voltage by 90° since it is a purely reactive current and does not contribute directly to no-load losses [7-8]. In Fig. 1, R_{W1}, L_{l1}, and C_{P1} are the winding resistance, leakage inductance, and parasitic capacitance for the primary side, respectively.

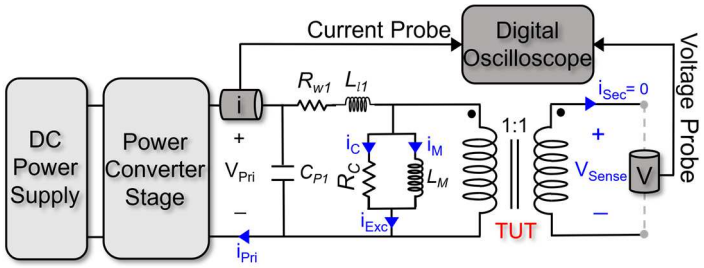

Fig. 1: Two-winding method for measuring the HF transformer core loss under the no-load conditions.

The core loss of the HF Transformer under test (TUT) is acquired by measuring the area of a closed *B–H* loop or integrating the product of the open-circuit voltage drop across the secondary winding (sensing winding, V_{Sense}) and the excitation current as defined in (1)

$$P_{Core} = \frac{N_1}{N_2}\frac{1}{T}\int_0^T i_{Exc}(t)\cdot v_{Sense}(t)\,dt \tag{1}$$

where T is the period of one cycle; $N1$ and $N2$ are the numbers of the primary and secondary winding turns, respectively. For simplicity of the loss calculation, by putting the equal turn ratios (1:1), the transformer has the same number of turns on each coil ($n = N_1/N_2 = 1$). The waveform signals are captured by the probes and digital oscilloscope over time as shown in Fig. 1.

In this paper for measuring the core loss, the TUT is excited with a bidirectional half-bridge structure proposed before in the former studies as [2-3]. By adjusting the output voltages of the two DC power supplies utilized in the half-bridge circuit, the asymmetric rectangular voltage generated by the device voltage drops can be compensated. Hence, this modification contributes to having a closed *B-H* loop, due to the consuming equal energies by the positive half cycle and the negative half cycle of the symmetric voltage excitation. If the magnetization or demagnetization process can not be completely finalized, it causes the unclosed *B-H* trajectory, which has the consequences of incorrect loss computation [17]. To excite the TUT, a refined discontinuous test procedure as a triple pulse test (TPT) is applied, presented before in [2-3]. To avoid unnecessary full-time operations and temperature rise, the TPT concept is formed, which operates only the necessary cycles and accelerates the estimation process. With the utilization of high-bandwidth voltage and current probes, a test rig has been built in the form of a two-winding method to experience TPT for measuring core loss. The test rig is depicted in Fig. 2, and the components and instruments in the test rig are listed in Table I.

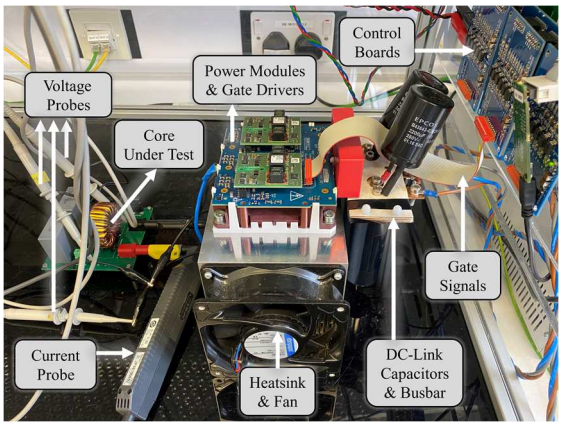

Fig. 2: The utilized test rig of the TUT core loss measurement.

TABLE I: COMPONENTS AND INSTRUMENTS IN THE TEST RIG

Power Supplies	Elektro-Automatik TS 8000 T
Voltage Probe	Keysight N2862B (150 MHz)
Differential Probe	Pico TA041 (25MHz)
Current Probe	Keysight N2783B (100 MHz)
Power Module	Semikron SKiM301TMLI12E4B
Gate Driver	Semikron SKYPER 42 J
Digital Oscilloscope	MSO-X 3054A (500 MHz, 4 GSa/s)
DC-Link Capacitance	*C1* = *C2* =2670 µF
Tested component	92 µH, T184-26, Micrometals©, *N1*:*N2*=24:24

As a result of square voltage excitation, the TUT observes the actual waveform that is emulated by TPT in the test setup. The experimental waveforms shown in Fig. 3 is illustrated a TPT procedure for one test point at the frequency of 10 kHz for the TUT presented in Table I in the no-load condition. The amplitude of the testing (V_{Pri}) is stabilized to half the dc-link voltage, which is 50 V at this test point. The selected cycle is chosen for calculating the core loss when the system has reached to steady-state and the waveforms are fixed. As a result, the closed *B-H* loop can be expected. A digital oscilloscope and software used for post-processing such as MATLAB are used to calculate the core loss through the selected cycle. In order to reduce phase discrepancy error, the voltage/current probe is aligned using Keysight U1880A deskew tool and calibrated on the oscilloscope with the deskew function. The core loss calculated for the target cycle of the testing point in Fig. 3 is 4.35 mJ, which can be obtained by (1) in the no-load condition. A short testing transition prevents any temperature rise in the TPT which makes it easy to control. Hence, all experiments presented in this article are performed at room temperature (T = 25°C).

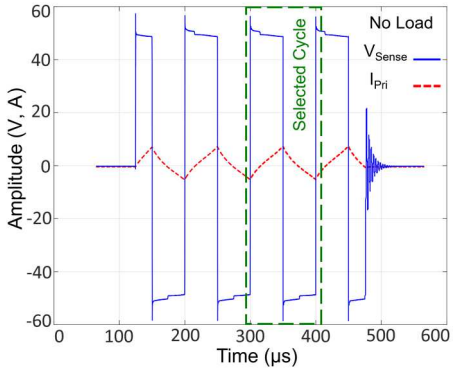

Fig. 3: Experimental current/voltage waveforms of one TPT test point for the no-load condition at 10 kHz and V_{Pri} = 50 V.

B. Loaded Condition

In this section, the load is added to the secondary winding of the HF transformer as shown in Fig. 4, to examine the differences between the loaded and no-load conditions of the transformer's core losses. Two various film resistors, i.e. 4 Ω and 8 Ω with low intrinsic parasitic inductance ($L_{Load} \approx 20$ nH), are selected to further demonstrate the differences between the loaded core loss results. Instead of using the secondary winding, auxiliary winding with the same number of turns equal to the primary and secondary sides is used to measure the voltage across the magnetizing inductance as V_{Sense}, to cancel out the voltage drops caused by the secondary side load resistor (R_{Load}), secondary winding resistance (R_{W2}) and leakage inductance (L_{l2}).

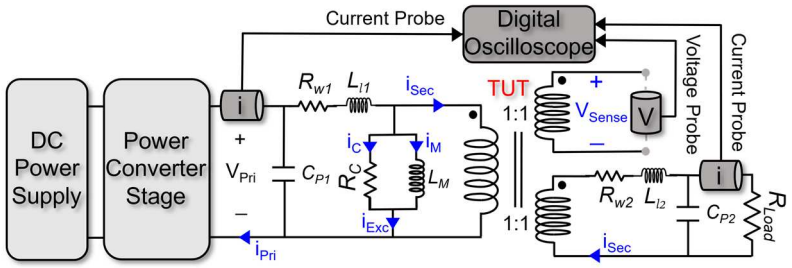

Fig. 4: Two-winding method for measuring the HF transformer core loss under the loaded conditions.

Fig 5 displays the TPT voltage and currents waveforms of the TUT presented in Table I for the 4 Ω and 8 Ω load resistors at the frequency of 10 kHz.

To measure the core loss in loaded conditions, the excitation current is needed, while it is not equal to the primary current to effortlessly attained similar to the no-load condition. The i_{Exc} can be achieved indirectly by subtracting the primary current from the secondary current when the turn ratio is equal to one (n = 1) [7].

$$i_{Exc} = i_{Pri} - \frac{i_{Sec}}{n} \tag{2}$$

As a result, the core losses can be calculated for the selected cycles in Fig. 5 by (1), which are 3.85 mJ and 3.92 mJ for 4 Ω and 8 Ω load resistors, respectively. The obtained loaded core loss values are not equal to the core loss value measured from the no-load condition in the previous section. Nevertheless, it was assumed that the presence of load would not change the core loss value considerably in different load conditions. To better investigate and clarify why the three attained core losses are different from each other, the obtained V_{Sense} and i_{Exc} waveforms for three different load conditions are shown in Fig 6.

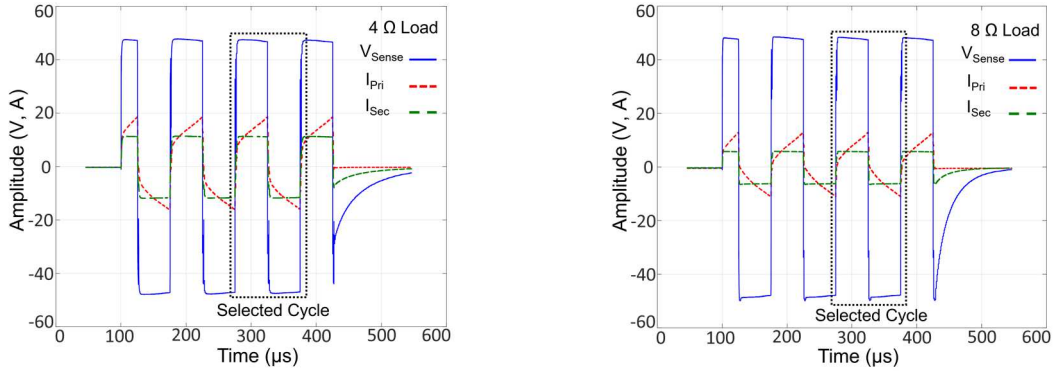

(a) (b)

Fig. 5: Experimental currents/voltage waveforms of one TPT test point at 10 kHz and V_{Pri} = 50 V for the (a) 4 Ω and (b) 8 Ω load resistors.

Fig. 6 illustrates that the amplitude of the sensed voltage is changed with different load conditions. By reducing the load resistance from an open-circuit condition (assuming the lightest load resistance), or increasing the primary and secondary currents, it appears that the sensed voltage has decreased. However, for the excitation current cases in Fig. 6 (b), it is difficult to accurately investigate the current waveforms distinctions from the figure under varied load values compared to the no-load condition, due to the small values. By calculating the differences between the measured voltages and currents for different load conditions in Fig. 6, Fig. 7 depicts the results in more detail.

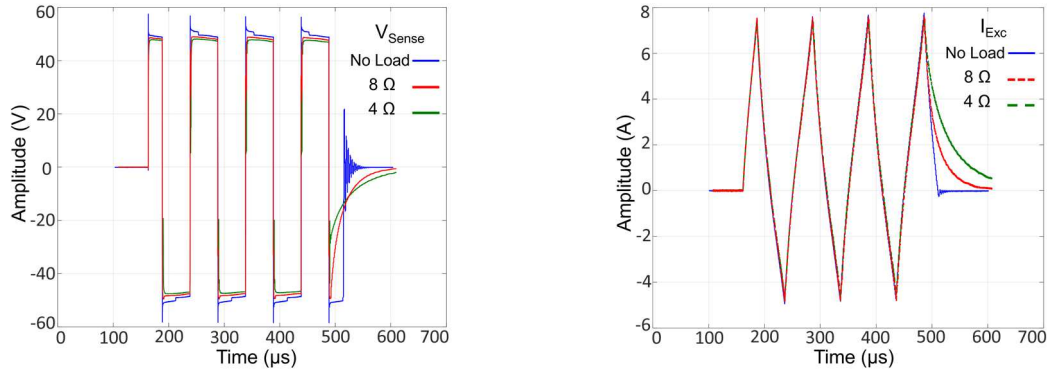

(a) (b)

Fig. 6: Experimental waveforms of the various load conditions at 10 kHz and V_{Pri} = 50 V for the (a) sense voltages and (b) excitation currents.

According to Fig. 6 (a) and Fig. 7 (a), the sensing voltage amplitudes of loaded conditions are lower than the no-load test. In addition, the sense voltage amplitude of the 4 Ω load resistor is around 1 V lower compared to the 8 Ω load case. For the excitation current case, in Fig. 7 (b), there is a small amplitude difference between the loaded and no-load conditions. Similar to the sensed voltages, the higher load resistance values have resulted in more excitation current. Also, between the two cases of 8 Ω and 4 Ω excitation currents, there is around a 0.1 A amplitude dissimilarity. A higher sensed voltage amplitude suggests the presence of additional electromagnetic fields within and around the windings and core in higher load resistance conditions. Also, these results are indicated that there are more voltage drops across the winding of the loaded conditions. Furthermore, a higher excitation current proposes that one or both of the i_C and i_M has changed according to Fig. 4, which can lead to a more core loss. Consequently, as it is shown, the measured waveforms for computing the core loss may differ between

the no-load and loaded conditions for the HF transformers. Variation in these parameters can be a key reason and reveal why the core loss is varied with various load conditions.

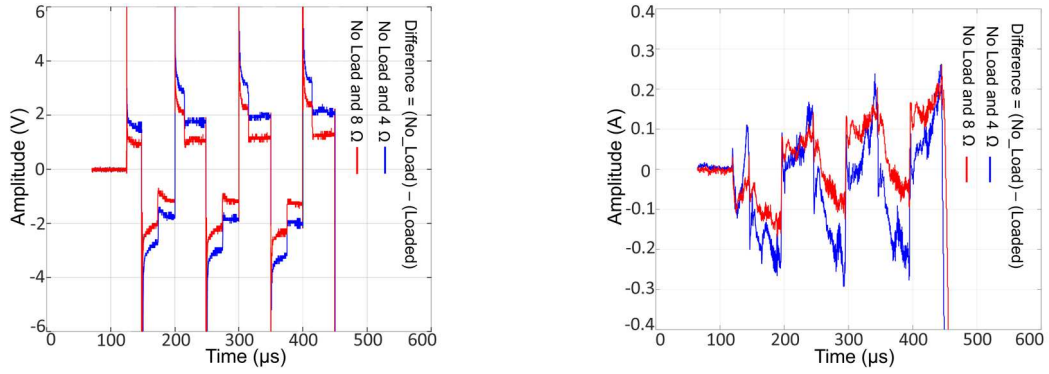

(a) (b)

Fig. 7: Differences between the experimental waveforms of various loaded conditions compared to the no-load condition for the (a) sense voltages and (b) excitation currents.

The simplified equivalent circuit of the HF transformer referred to the primary side is shown in Fig. 8. The parasitic capacitances for the primary and secondary sides can be ignored due to their negligible values [10]. Since n=1, the impedance values of the transferred parameters to the primary side are kept constant. If the V_{Pri} is fixed to a certain voltage, by assuming constant primary and secondary winding impedances, R_C, and L_M, and increasing the load resistance value, both the primary and secondary currents decrease. Equations (3) and (4) are the results of the KVL over the closed-loop between the primary and secondary sides of the TUT and the magnetizing inductance in Fig. 8, respectively. According to (3), when the I_{Pri} increases at heavier loads, the voltage drop across the primary winding resistance and leakage inductance are increased which leads to a decrement of the V_{Sense}. Additionally, equation (4) demonstrates that by falling the secondary current at lighter loads, the V_{Sense} is also reduced.

$$V_{Sense} = V_{Pri} - I_{Pri}(R_{W1} + L_{l1}) \tag{3}$$

$$V_{Sense} = I'_{Sec}(R'_{W2} + L'_{l2} + R'_{Load}) \tag{4}$$

Therefore, one of the main reasons that change the sensed voltage is the voltage drops across the parasitic elements such as winding resistance and leakage inductance of the HF transformer at different load conditions owing to the variation of the windings' current. To sum up, the voltage that the magnetizing inductance needs to be excited will be reduced at heavier loads due to the voltage drops caused by the parasitic elements. Since the L_M had assumed to be constant, when the V_{Sense} is changed, the i_{Exc} is also varied as depicted in Fig. 7.

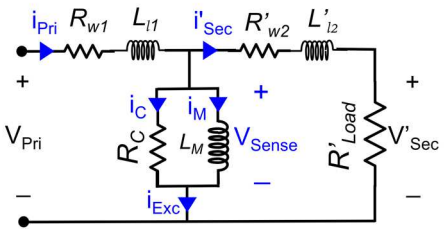

Fig. 8: Equivalent circuit of HF transformer for the loaded conditions with secondary parameters referred to the primary.

Enlargement of the V_{Sense} can result in an increment of the flux density (B) as well as flux density swing (ΔB) and subsequently change the core loss, as the core loss is generated by the varying magnetic flux field within a material. Fig. 9 (a) shows the obtained experimental ΔB of the TUT in various load conditions and excitation frequencies. In this figure, the applied TUT voltage, V_{Pri}, is held constant to 50 V regardless of the frequency increment, which is resulted in the reduction of flux density swings at higher frequencies. The no-load condition has a higher ΔB compared to the loaded conditions, and by reducing the load value, the ΔB is also decreased. By assuming the no-load ΔB result as a reference value, the differences between the loaded conditions and the no-load case are displayed in Fig. 9 (b). It can be seen that the mismatches are slightly increased when the frequency grows, which is more

considerable for the heavier load value. The increase of the mismatches at higher frequencies is owing to the increment of the winding resistance and inductive leakage reactance. Also, since the 4 Ω load condition has higher windings currents, its voltage drops and mismatches from the no-load condition are more compared to the 8 Ω load condition. Variation in flux density at various load conditions confirms one of the main reasons that lead to a change in the core loss which can be caused by the voltage drops of the parasitics elements.

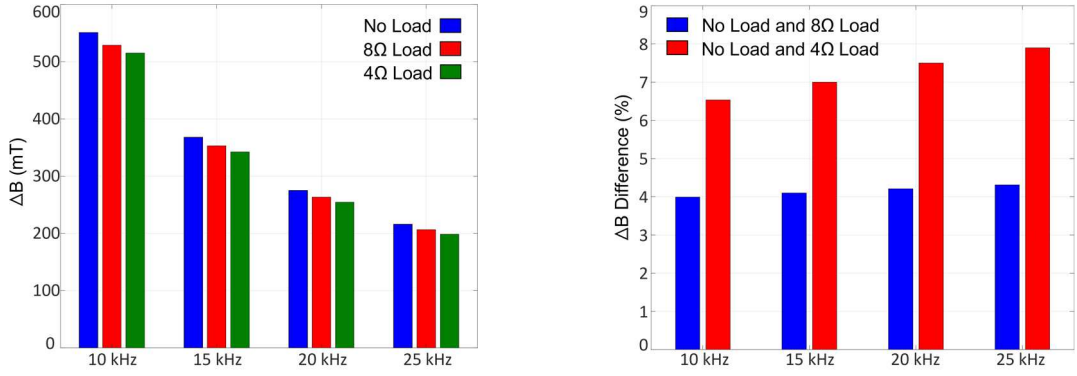

(a) (b)

Fig. 9: (a) Experimental flux density swing of the TUT for various load conditions and excitation frequencies at V_{Pri}=50 V, (b) the differences between the loaded conditions and no-load when the no-load result considers as a reference value.

Fig. 10 (a) depicts the obtained TUT core losses at various frequencies for different load conditions. Similar to the flux density swings in Fig. 9, the core loss is decreased at heavier loads and these differences are intense at higher frequencies. For instance, as depicted in Fig. 10 (b), the difference between the no-load and 4 Ω load conditions at 10 kHz when the no-load result considers as a reference value is around 11.5 %; however, this difference is increased to about 16 % at 25 kHz.

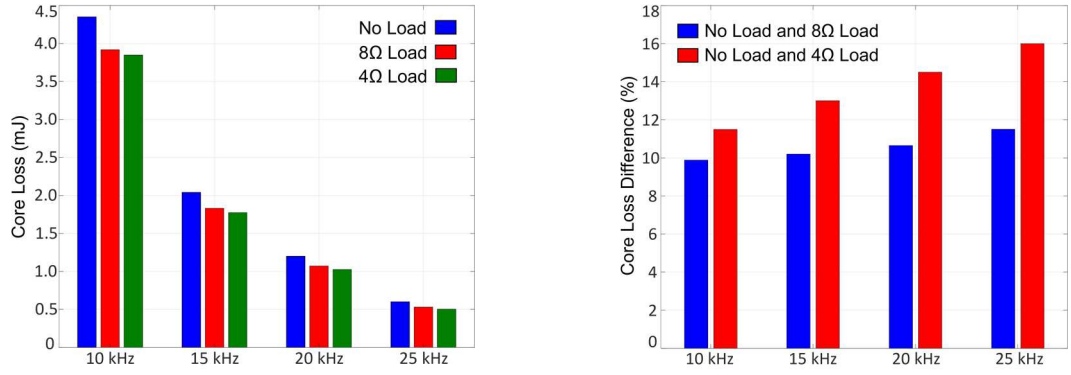

(a) (b)

Fig. 10: (a) TUT core losses at various frequencies for different load conditions when V_{Pri} = 50 V, (b) the core loss differences between the loaded conditions and no-load when the no-load result considers as a reference value.

III. Finite Element Analysis (FEA) Evaluation

To entirely realize the causes of the core loss variation under different load conditions, the FEA analysis is employed. The HF transformer used in the experiment (Table I) is simulated through 3D ANSYS Maxwell and depicted in Fig. 11 (a). Fig. 11 (b) and (c) illustrate the magnetic flux density of the core for the no-load and 0.1 Ω load conditions at 10 kHz when the voltage and the magnetic flux density are at peak value (V_{Pri} = 50 V). The 0.1 load resistor is chosen to better compare the two conditions of lightest load, i.e. open circuit condition, and heaviest load condition which is similar and close to the short circuit test. The 0.1 Ω load condition has a small magnetic flux density and core loss as depicted in Fig. 11 (c) since the magnetizing inductance is almost shorted out and mainly the leakage inductance remained in the circuit. Hence, from Figs. 11 (b) and (c) can be concluded that the load condition plays an important role in the magnetic flux density of the core and core loss as well.

The core loss is computed through the FEA analysis and shown in Fig. 12 (a). There is around a 5% difference between the simulation and experimental method when the empirical result is considered as

a reference value. For several reasons, the FEA captures a higher core loss than the experiment results. The main one is that Ansys Maxwell [18] uses the cores datasheet to compute the core loss which is based on the sinusoidal excitation. With the same magnitude of the flux density, normally the sinusoidal excitation has higher core loss compared to the square waveform excitation when the duty cycle is equal to 50% [19]. In the other duty cycles, the core loss starts to increase and more deviate from sinusoidal excitation as there are more intense high order harmonics included compared to the 50% case. In addition, it is not possible to completely and precisely simulate and replicate the TUT similar to the actual geometrical structure of the component considering the shape and winding configuration, especially when TUT is randomly wound.

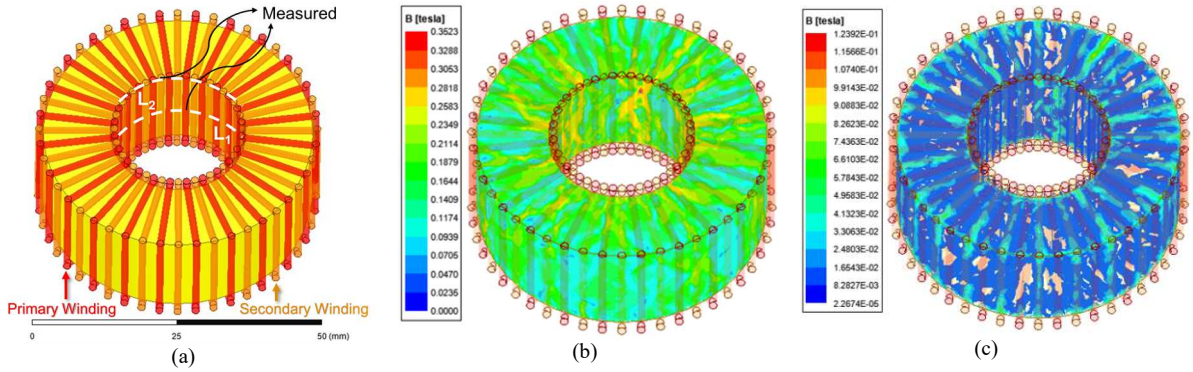

(a) (b) (c)

Fig. 11: (a) The FEA simulation model of the utilized HF transformer, (b) the magnetic flux density for the no-load condition at 10 kHz when V_{Pri} = 50 V, (c) the magnetic flux density for the 0.1 Ω load condition at 10 kHz when V_{Pri} = 50 V.

Fig. 12 (b) shows the FEA core loss results for different load conditions and the difference between the loaded and no-load conditions when the no-load core loss consider as a reference value. The difference between the 100 Ω load and 1 Ω load resistors compared to the no-load condition are around 6% and 16%, respectively. Fig. 12 confirms that similar to the results obtained in the previous empirical section, the core loss is changed with different load conditions, which is reduced from no-load to heaviest load conditions.

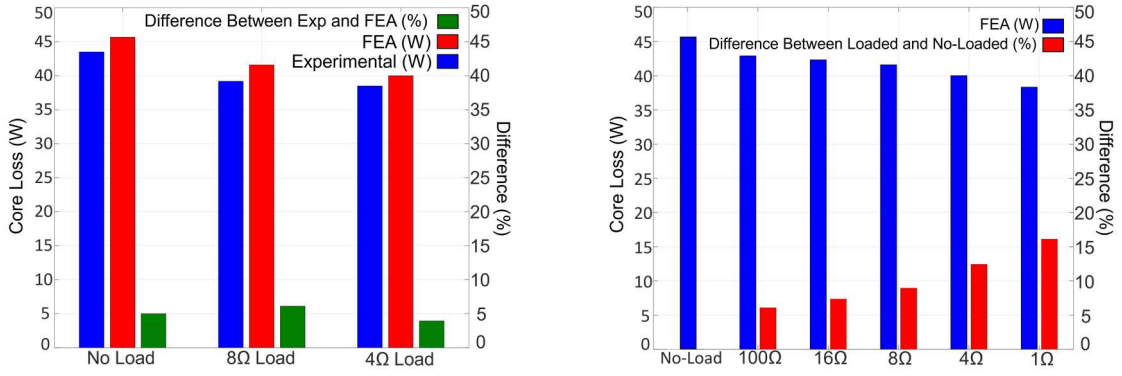

(a) (b)

Fig. 12: (a) The obtained core losses from the FEA and experiment at 10 kHz and V_{Pri} = 50 V, (b) the FEA core loss and the difference between the loaded and no-load conditions when the no-load core loss is considered as a reference value at 10 kHz when V_{Pri} = 50 V.

Fig. 13 (a) demonstrates the magnetic flux density of the core for the two cases of no-load and 0.1 Ω load resistor for the middle line (L_1) depicted in Fig. 11 (a). The L_1 is at the middle of the toroidal core surface (throughout the inner circle of the core) and its length is equal to about 75 mm regarding the core specifications. Fig. 13 (a) shows the magnetic flux density at 10 kHz when the voltage is at peak value (V_{Pri} = 50 V), for each point of the L_1 length, which clarifies a large gap between the two different very high and low load conditions.

By calculating the average value of magnetic flux densities for the whole length of the two L_1 and L_2 lines shown in Fig. 13 (a), Fig. 13 (b) illustrates the average magnetic flux density (B_{Avg}) during the time. The L_2 line is selected to properly investigate the influence of the end/edge-winding leakage flux on the edge of the core region, where the presence of the windings is more concentrated compared to

the other parts of the core. For the two load cases as no-load and 1 Ω load conditions and for both the L_1 and L_2 lines, the B_{Avg} of the no-load condition has higher peak values in contrast to the 1 Ω load resistor. Additionally, the B_{Avg} of the L_2 for both load conditions are higher than the L_1, which is confirmed the excessive amount of local flux density variation in the edge of the core region.

Fig. 13 (c) shows the difference between the B_{Avg} of the no-load and 1 Ω load cases for the L_1 and L_2 ([B_{Avg} at No-load] – [B_{Avg} at 1 Ω]). At some points, this difference is less than zero because the no-load magnetic flux density is lower than the 1 Ω load case. However, the magnetic flux density of the no-load case is overall higher than the 1 Ω load resistor condition since the mean value of the L_1 case is 9.5 mT and for L_2 is 10.8 mT in Fig. 13 (c), which are both higher than zero. Also, it can be observed that the difference for the L_2 is higher than the L_1 for about 1.3 mT.

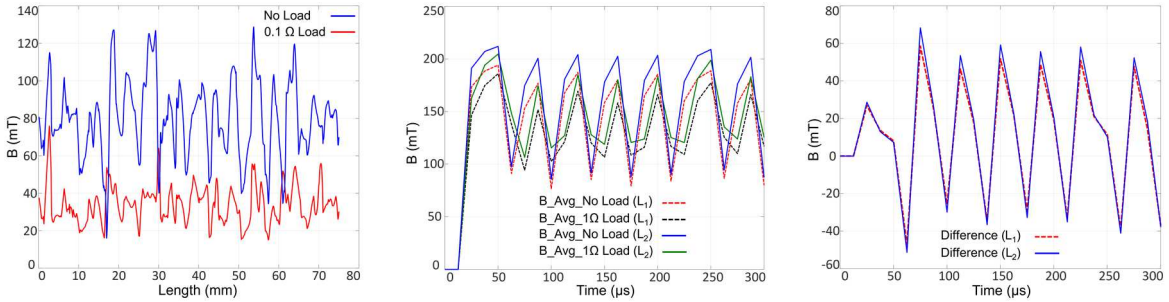

(a) (b) (c)

Fig. 13: (a) the magnetic flux density of the core for no-load and 0.1 Ω load resistors for the L_1 at voltage peak value, (b) the B_{Avg} for the two L_1 and L_2 lines at different load conditions, (c) the difference between the B_{Avg} of the no-load and 1 Ω load cases for the L_1 and L_2.

Fig. 13 clarifies that for the heavier loads, the B_{Avg} is lower compared to the light loads. Besides, the magnetic flux density in the edge of the core region is higher compared to the middle part. As explained, changing the AC resistance can influence the end/edge-winding leakage flux, and causes a local flux density variation in the edge of the core region, which leads to a change in the core loss value. Fig. 14 shows the AC resistance of the HF transformer winding, which is obtained by FEA analysis for different load conditions. Both the primary and secondary windings of the studied transformer have the same self-resistance value as they have the same number of turns and specifications. When the load impedance value is reduced (or the windings currents are increased), the HF transformer's windings resistance value is also decreased. The winding resistance value reduction is owing to the proximity effect and increasing the mutual resistance between the primary and secondary windings of the HF transformer [11-12]. Consequently, the higher resistance value at higher load conditions can be one of the factors of higher core loss, since the local magnetic flux density in the edge of the core region increases and causes more core loss. This also implies that the core loss value can alter considerably during the loaded conditions owing to the winding resistance and current amplitude variations.

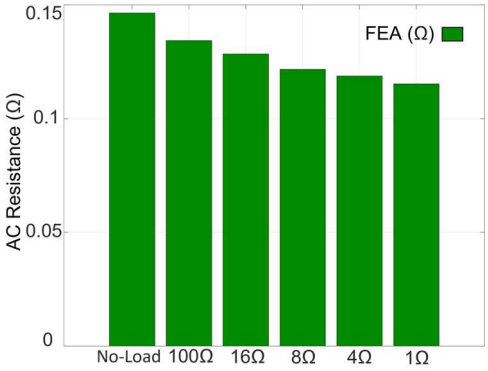

Fig. 14: The winding AC resistance of the HF transformer at different load conditions.

IV. Conclusion

The core loss of the HF transformers is previously assumed to be constant at different load conditions and measured experimentally with a no-load test. This paper demonstrates that the various load

conditions can affect the core loss in HF transformers due to the variation of winding parasitics elements and subsequently the transformer's excitation voltage and current waveforms, and the field interactions between the primary and secondary windings and between the windings and core. It is concluded that a heavier load results in a lower core loss, due to the lesser value of the magnetic flux density in the core, and more voltage drops across the parasitic elements of the winding. The captured experimental results are compared with the three-dimensional (3D) finite element analysis (FEA) results conducted in Ansys Maxwell, to provide a comprehensive evaluation.

References

[1] Y. Han and Y. Liu, "A practical transformer core loss measurement scheme for high-frequency power converter," in *IEEE Transactions on Industrial Electronics*, vol. 55, no. 2, pp. 941-948, Feb. 2008.

[2] J. Wang, K. J. Dagan, X. Yuan, W. Wang and P. H. Mellor, "A Practical Approach for Core Loss Estimation of a High-Current Gapped Inductor in PWM Converters With a User-Friendly Loss Map," in *IEEE Transactions on Power Electronics*, vol. 34, no. 6, pp. 5697-5710, June 2019.

[3] J. Wang, X. Yuan and N. Rasekh, "Triple Pulse Test (TPT) for Characterizing Power Loss in Magnetic Components in Analogous to Double Pulse Test (DPT) for Power Electronics Devices," *IECON 2020 The 46th Annual Conference of the IEEE Industrial Electronics Society*, 2020, pp. 4717-4724.

[4] J. Wang, N. Rasekh, X. Yuan and K. J. Dagan, "An Analytical Method for Fast Calculation of Inductor Operating Space for High-Frequency Core Loss Estimation in Two-Level and Three-Level PWM Converters," in *IEEE Transactions on Industry Applications*, vol. 57, no. 1, pp. 650-663, Jan.-Feb. 2021.

[5] J. Muhlethaler, J. Biela, J. W. Kolar and A. Ecklebe, "Core Losses Under the DC Bias Condition Based on Steinmetz Parameters," in IEEE Transactions on Power Electronics, vol. 27, no. 2, pp. 953-963, Feb. 2012.

[6] B. X. Foo, A. L. F. Stein and C. R. Sullivan, "A step-by-step guide to extracting winding resistance from an impedance measurement," *2017 IEEE Applied Power Electronics Conference and Exposition (APEC)*, 2017, pp. 861-867.

[7] K. K. Marian, High-frequency magnetic components, 2nd ed. Chichester: WILEY, 2014.

[8] Mehta, V. K., Rohit Mehta, Objective Electrical Technology: For the Students of U.P.S.C. (Engg. Services), I.A.S. (Engg. Group), B. Sc. (Engg.), Diploma and Other Competitive Courses: Over 2800 Objective Questions with Hints. Ram Nagar, New Delhi: S. Chand, 2010.

[9] V. Karthikeyan, S. Rajasekar, S. Pragaspathy and F. Blaabjerg, "Core Loss Estimation of Magnetic Links in DAB Converter Operated in High-Frequency Non-Sinusoidal Flux Waveforms," *2018 IEEE International Conference on Power Electronics, Drives and Energy Systems (PEDES)*, 2018, pp. 1-5

[10] N. Rasekh, J. Wang and X. Yuan, "A Novel In-Situ Measurement Method of High-Frequency Winding Loss in Cored Inductors With Immunity Against Phase Discrepancy Error," in *IEEE Open Journal of the Industrial Electronics Society*, vol. 2, pp. 545-555, 2021.

[11] J. H. Spreen, "Electrical terminal representation of conductor loss in transformers," in *IEEE Transactions on Power Electronics*, vol. 5, no. 4, pp. 424-429, Oct. 1990.

[12] E. L. Barrios, D. Elizondo, A. Ursúa and P. Sanchis, "Winding Resistance Measurement in Power Inductors - Understanding the Impact of the Winding Mutual Resistance," in *IEEE Access*, vol. 9, pp. 92224-92238, 2021.

[13] A. Al-Timimy, P. Giangrande, M. Degano, M. Galea and C. Gerada, "Investigation of AC Copper and Iron Losses in High-Speed High-Power Density PMSM," *2018 XIII International Conference on Electrical Machines (ICEM)*, 2018, pp. 263-269

[14] C. Feeney, J. Zhang and M. Duffy, "AC Winding Loss of Phase-Shifted Coupled Windings," in *IEEE Transactions on Power Electronics*, vol. 31, no. 2, pp. 1472-1478, Feb. 2016.

[15] V. J. Thottuvelil, T. G. Wilson, and H. A. Owen, "High-frequency measurement techniques for magnetic cores," *IEEE Trans. Power Electron.*, vol. 5, no. 1, pp. 41–53, Jan. 1990.

[16] N. Rasekh, J. Wang and X. Yuan, "A New Method for Offline Compensation of Phase Discrepancy in Measuring the Core Loss With Rectangular Voltage," in *IEEE Open Journal of the Industrial Electronics Society*, vol. 2, pp. 302-314, 2021.

[17] T. Shimizu and S. Iyasu, "A practical iron loss calculation for AC filter inductors used in PWM inverters," *IEEE Trans. Ind. Electron.*, vol. 56, no. 7, pp. 2600–2609, Aug. 2009.

[18] ANSYS Maxwell, Oct. 2021. [Online]. Available: https://www.ansys.com/products/electronics/ansys-maxwell

[19] M. Mu and F. C. Lee, "A new core loss model for rectangular AC voltages," 2014 IEEE Energy Conversion Congress and Exposition (ECCE), 2014, pp. 5214-5220.